Stability Analysis of a Drop Generation from a Nozzle in an Electric Field with Corona Discharge

Kazuyuki Tada and Hiroyuki Kawamoto; Department of Applied Mechanics and Aerospace Engineering, Waseda University, Shinjuku, Tokyo, Japan

Abstract

Stability of a conducting drop hanging from a nozzle in an electric field with corona discharge was examined theoretically for the first time. By this static model with linear stability analysis, stability of electrostatic inkjet process was estimated. The basic equations, the augmented Young-Laplace equation for drop shape and the Poisson equation for electric field, were coupled and solved by the Finite Element Method. According to the initial condition of its shape, a drop is deformed and subject to corona discharge with the increment of non-dimensional electric field. It was found this static model was applicable to estimate the range of stable jetting and the existence of corona discharge reduces its stable jetting range.

Introduction

Since the first inkjet printer, gMingographh appeared in market from Seimens Co., Ltd.[1][2], the inkjet technology has progressed tremendously in quality and print speed. Although the electrostatic inkjet technology has not applied to commercial printers, it is attractive in the industrial application. It can make various forms of jet, such as individual drop (drop on demand)[3], micro spray[4] or spindle[5] that could be utilized to make fibers. Additionally, it could jet highly viscous liquid[6] and make such a super fine drop as less than 1 femto litter[3]. Fundamental understaining is indispensable to apply this technology to industrial usages so that the stability of an electrified drop hanging from a nozzle was examined theoretically. Although the jetting is a dynamic process, it was found that the electro-hydrostatic approach including linear stability analysis was useful to estimate the range of stable jetting.

Without corona discharge, several authors reported the effect of electrostatic field on a drop hanging from a nozzle[7]-[12]. Although the corona discharge occurs sometimes inevitably especially in the nozzle-to-plate geometry, the theoretical study is limited to calculate the electrostatic field[13]. Providing the fundamental model related to electrostatic inkjet phenomena with corona discharge is the goal of this research.

Theoretical Model

Calculation Domain

Fig.1 shows an axisymmetric, conducting drop hanging from a nozzle of length H_2. The nozzle is at potential u_0 and the bottom plate, a distance H_1 from the tip of the nozzle, is grounded. L is length between the axis of the nozzle and asymptotic boundary of calculation domain. The z-axis is parallel to gravity and the horizontal plane $z = 0$ is located at the tip of the nozzle.

Two coordinate systems are used with the origins of both systems located in the plane $z = z_c$ along the axis of symmetry. A

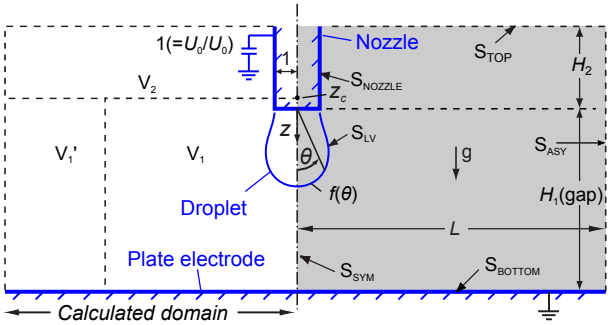

Figure 1. *Pseudo-electrostatic inkjet model: a drop hanging from a nozzle in an axisymmetric pin-to-plate system. S_{NOZZLE}:surface of nozzle, S_{BOTTOM}:surface of plate electrode, S_{LV}:surface of a droplet, S_{SYM}:surface of symmetric plane, S_{TOP}, S_{ASY}:surface of calculation boundary, V_1:calculation domain, spherical-coordinate area, V_1', V_2:calculation domain, cylindrical-coordinate area.*

spherical coordinate system (r, θ, ϕ) is applied to the domain V_1 where r is the radial coordinate and θ and ϕ are the meridional and azimuthal angles, respectively. A cylindrical coordinate system (x, ϕ, z), where x is the projection of r onto the plane $z = z_c$, is applied to all other domains. Because an unbounded domain is impracticable, the length L must be finite. To reduce the influence of the length L, cylindrical coordinate domain V_1' is added to the domain V_1.

Governing Equations and Boundary Conditions

The equilibrium shape of an inviscid and conductive drop hanging from a nozzle is governed by the augmented Young-Laplace equation (eq.(1)) on the interface between the drop and the ambient fluid (air)[7][8]. With corona discharge, the electrostatic pressure is governed by non-linear differential equation, the Poisson equation(eq.(2)) and the conservation of charge(eq.(3)).

$$\nabla_s \cdot \boldsymbol{n}_{LV} = K + G + NeE_n^2 \tag{1}$$

$$\nabla^2 u = -\rho_E \tag{2}$$

$$\nabla \cdot \rho_E \nabla u = 0 \tag{3}$$

where all the paramters in above equations are dimensionless. Lengths are measured in unit of $\tilde{R}$, radius of nozzle and potential is in unit of $\tilde{u}_0$, applied voltage, i.e. $\nabla \equiv \tilde{R}\tilde{\nabla}$, $u \equiv \tilde{u}/\tilde{u}_0$. Those parameters with/without tilde above them are dimensional/dimension-less respectively. Reference pressure $K(\equiv R\Delta\tilde{p}_0/\sigma)$ is the pressure difference $\Delta\tilde{p}_0$ between the drop

and the ambient air. $E_n(\equiv \tilde{R}\tilde{E}_n/\tilde{u}_0)$ denotes the normal component of the electric field. $\rho_E(\equiv \tilde{\rho}_E\tilde{R}^2/\varepsilon\tilde{u}_0)$ is the charge density. $\boldsymbol{n}_{LV}$ is the unit normal vector of the drop surface. Two dimensionless numbers are defined; electrical Bond number as $Ne(\equiv \varepsilon\tilde{u}_0^2/2\tilde{\sigma}\tilde{R})$ and gravitational Bond number as $G(\equiv g\tilde{R}^2\Delta\tilde{\rho}/\tilde{\sigma}$, $\Delta\tilde{\rho}$:the difference of density between droplet and air, $\tilde{\sigma}$:surface tension). A drop is so small that the gravitational Bond number is negligible ($G=0$). Reference pressure K is set by constraining the drop volume to be a fixed amount V_0.

$$V = V_0 \tag{4}$$

To search for the turning points (TP) where the system changes from stable region to unstable region by linear stability analysis, another relation is defined which specifies an adaptive choice of parameter P[14].

$$P = P_0 + \Delta P \tag{5}$$

The above equations are solved subject to following boundary conditions,

$$\begin{aligned} &f_\theta \equiv df/d\theta = 0 \quad \text{at } \theta = 0 \\ &f = 1 \quad \text{at } \theta = \pi/2 \end{aligned} \tag{6}$$

$$\begin{aligned} &u = 1 \quad \text{on } S_{LV} \text{ and } S_{NOZZLE} \\ &u = 0 \quad \text{on } S_{BOTTOM} \\ &\boldsymbol{n}\cdot\nabla u = 0 \quad \text{on } S_{SYM}, S_{ASY} \text{ and } S_{TOP} \end{aligned} \tag{7}$$

where f is the distance between drop surface and the origin of coordinate, z_c. The boundary condition related to corona discharge is as follows,

$$E_n \le E_0 \quad \text{on } S_{LV} \tag{8}$$

where E_0 is the critical electric field on the drop surface where corona discharge occures. It is supposed that the electric field is independent to the applied voltage, kept constant to $E_0(\tilde{E}_0 = 14.55\times10^6 V/m$[13]) above the critical applied voltage where corona discharges.

Numerical analysis

The domain is tessellated into a set of quadrilateral elements, as shown in Fig.2. In the domain V_1 the elements are bordered by the fixed spines in r-direction and by the curves in θ-direction, which move proportionally to the free surface along the spines [15]. Because the domain is axisymmetric, only the domain of positive x-direction is calculated.

Fig.3 is the flow chart of this numerical method. At first the calculation starts at low voltage (i.e. $Ne=0$) below the critical voltage where corona discharges. Uniform and small value is assumed for the initial condition of charge densty ($\rho_0 = 10^{-10}$). Next, eq.(1),eq.(2),eq.(4) and eq.(5) are coupled and electric potential, u_1 and others are solved by the Galerkin Finite Element Method (GFEM) with the boundary conditions, eq.(6)-eq.(8). When the electric field at some nodes on the droplet surface surpass the critical electric field, the electric field at the very node is forced (eq.(8)) to be E_0. Also, the other electric potential, u_2 is independently solved by GFEM with eq.(3) and the boundary

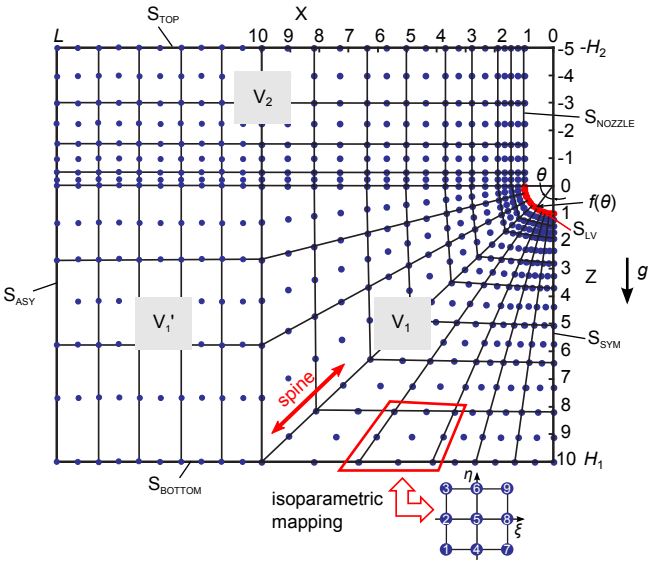

Figure 2. *Example of tessellated global domain and isoparametrically mapped local domain.*

condition eq.(8). From these two potentials, the stregths of electic field are calculated separately. The above calculations are repeated until criteria of convergence are satisfied with following correction of charge density in each calculation step.

$$\rho^{(k+1)} = \rho^{(k)}\left(1 + 2K_e\frac{E_2 - E_1}{E_2 + E_1}\right) \tag{9}$$

where k is the times of iteration and K_e is a constant ($K_e = 1.1$). If the calculation is converged and it is not reached to predetermined number of calculation cycle, parameter P is increased by the step size ΔP to obtain turning point (TP) by linear stability analysis. The method of choosing the parameter P is described below.

The eq.(1) and eq.(2) are coupled and solved by the Galerkin Finite Element Method (GFEM) simultaneously. Mutiplying eq.(1) and eq.(2) by weighting functions which are identical to the bi-quadratic basis functions and integrating them by parts, weak forms of the eq.(1) and eq.(2) are obtained as follows,

$$\begin{aligned} R_s^{YL} = &\int_{S_{LV}} \left[\nabla_s\cdot(\phi^s\boldsymbol{n}_{LV} - (K + G_Z + NeE_n^2)\phi^s\boldsymbol{e}_r\cdot\boldsymbol{n}_{LV}\right] dS_{LV} \\ &- \cos\theta_c \oint_{L_{LSV}} (\phi\ st_{LSV}\times\boldsymbol{n}_s\cdot\boldsymbol{e}_r) dL_{LSV} \quad \text{at } s = 1,\cdots,S \end{aligned} \tag{10}$$

$$\begin{aligned} R_i^p = &\int_V \left[\nabla\varphi^i\cdot\nabla u - \varphi^i\rho_E\right] dV_{LV} \\ &- \int_S \boldsymbol{n}\cdot\nabla\varphi^i dS_{LV} = 0 \quad \text{at } i = 1,\cdots,I \end{aligned} \tag{11}$$

where S and I denote numbers of nodes. Electric potential and drop shape are isoparametrically mapped onto the calculation domain[16] and expressed by the bi-quadratic basis functions as follows.

$$f(\theta) = \sum_{s=1}^{S} \beta_s\phi^s(\xi,\eta=0) \tag{12}$$

$$u(\theta,r)\ or\ u(z,x) = \sum_{i=1}^{I} \alpha_i\varphi^i(\xi,\eta) \tag{13}$$

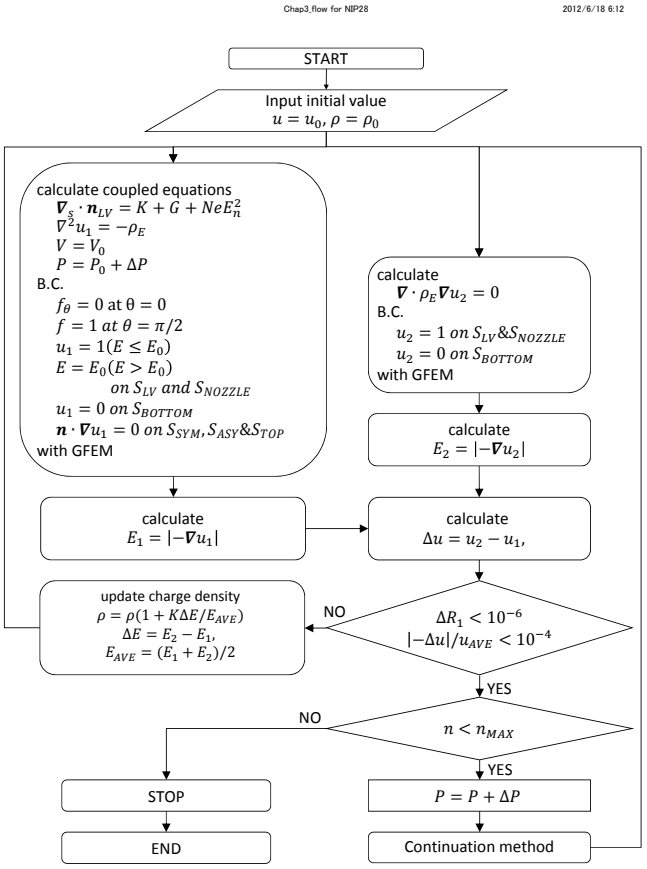

Figure 3. *Flowchart of numerical method*

So far, $N = S + I$ residuals and unknowns (β, α) are defined. The volume constraint eq.(4) is rewritten as the $N+1^{st}$ residual.

$$R_{N+1} \equiv R^{VC} = V - V_0 = 0 \tag{14}$$

$$R_{N+2} = P - P_0 - \Delta P = 0 \tag{15}$$

where P_0 is the value of the parameter at a known solution $\boldsymbol{\omega}^*$ on a family of solutions and the parameter step size ΔP is a specified increment to a new solution of $\boldsymbol{R}(\boldsymbol{\omega})$ on the same family. The paramter P is chosen from among $\boldsymbol{\omega}$ so that maximizes $\frac{\partial \omega}{\partial P}$) is maximized, i.e. P is the variable among the nodal values of free surface location and electrostatic potential, reference pressure and electrical Bond number whose value is changing most rapidly during continuation along solution family(Abott[14]). At the start of calculation the electric Bond number Ne is chosen as the parameter P. Finally the $N+2$ residuals and unknown vector are defined respectively as $\boldsymbol{R}(\boldsymbol{\omega}) \equiv (R^{VC}, R_{N+2}, \boldsymbol{R}^{YL}, \boldsymbol{R}^{P})$, $\boldsymbol{\omega} \equiv (K, Ne, \boldsymbol{\beta}, \boldsymbol{\alpha})$. The nonlinear sets of $N+2$ algebraic equations $\boldsymbol{R}(\boldsymbol{\omega}) = 0$ are solved simultaneously by Newton's method. With initial guess, $\boldsymbol{\omega}^{(0)}$, $k+1^{st}$ $(k = 1, 2, \cdots)$ solution can be solved as follows.

$$\boldsymbol{\omega}^{(0)}(P_0 + \Delta P) = \boldsymbol{\omega}^*(P_0) + \Delta P \frac{\partial \boldsymbol{\omega}}{\partial P}) \tag{16}$$

$$\underline{J}(\boldsymbol{\omega}^{(k)})(\boldsymbol{\omega}^{(k+1)} - \boldsymbol{\omega}^{(k)}) = -\boldsymbol{R}(\boldsymbol{\omega}^{(k)}) \tag{17}$$

where $\underline{J}$ is a Jacobian matrix. By applying boundary conditions eq.(8), eq.(17) is solved iteratively until the $L2$-norm of residuals

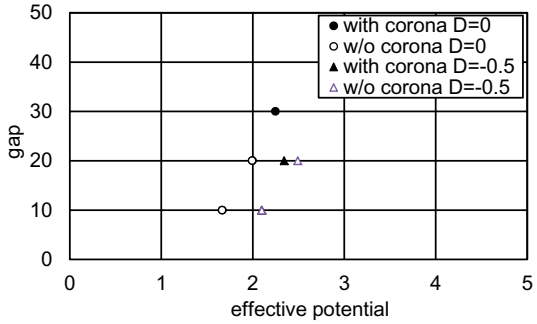

Figure 4. *Plot of turning points and gaps at* $G = 0$, $H_2 = 100$.

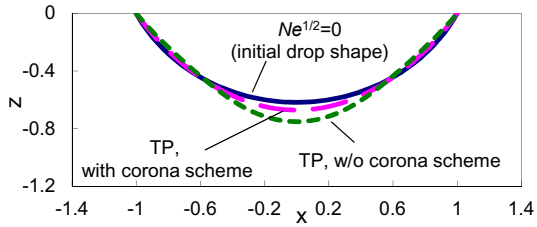

Figure 5. *Drop shapes at the turnig points.* $D = -0.5$, $gap = 20$.

$\boldsymbol{R}(\boldsymbol{\omega})$ were less than a prescribed tolerance. As quality of initial guess is critical for Newton method, follwoings were used as initial conditions because the equilibrium drop shapes are segments of spheres when gravitational and electrical forces are negligibly small compared to surface tension forces.

$$\begin{aligned} f^{(0)}(\theta) &= D\cos\theta + \sqrt{1 + D^2 - (D\sin\theta)^2} \\ U^{(0)}(\theta, r) &= \begin{cases} 0 & \text{everywhere in } V_1 \text{ and } V_2 \\ & \text{except on } S_{LV} \text{ and } S_{NOZZLE} \\ 1 & \text{on } S_{LV} \text{ and } S_{NOZZLE} \end{cases} \\ K^{(0)} &= 2 \\ Ne^{(0)} &= 0 \end{aligned} \tag{18}$$

Results

Fig.4 is the plot of the turning points in the case of the drop shape parameter $D = 0$ and $D = -0.5$ with or without the effect of corona discharge. It was already demonstrated that the turning points at $D = 0$ could estimate the jetting mode change from dripping mode to cone-jet mode[12]. As shown in Fig.4, in the case of $D = 0$, the effect of corona discharge is negligible, however, in the case of $D = -0.5$ and gap= 20, Fig.4 indicates that the corona discharge reduces the applied potential at the turning point as compared with the w/o-corona scheme. As is shown in Fig.5, the droplet in with-corona scheme become unstable although it deforms less than that in w/o-corona scheme. It can be estimated that the corona discharge reduces the applied potential to be unstable so that the region of stable region should be decreased. Further studies are indispensible for better understaing the corona effect in electrostatic inkjet phenomena.

Concluding remarks

Stability of a drop hanging from a nozzle in an electric field with corona discharge was examined theoretically. It was found that,

1. the static model with linear stability analysis was demonstrated to be applicable to estimate the range of stable jetting.
2. it seems that corona discharge enhances the instability of droplet so that the stable jetting region is reduced.

Although the foregoing results are equilibrium profiles provided that the drop volume is constant, they can suggest the way to achieve stable electrostatic inkjet process by introducing proper physical model such as corona discharge. Also they can be the guidance to the studies of dynamic phenomena.

References

[1] Webster Edward et al., INK JET PRINTING Its Role in Word Processing and Future Printer Markets (Published by DATEK of New England, (1980).

[2] Le, Hue P., Progress and Trends in ink-jet Printing Technology. J. Imaging Sci. Technol., Vol.42, No.1 (1998) pp.49-62.

[3] Murata, K., Super Fine Patterning by Using Inkjet Technology. J. J. Inst. Electronic Packaging, Vol.7, No.6 (2004) pp.487-490.

[4] Cloupeau, M., and Prunet-Foch, B., Electrostatic spraying of liquids: Main functioning modes. J. Electrostat., Vol.25 (1990) pp.165-184.

[5] Yamagata, Y., Matsumoto, H., Fabrication Technology of Nanofiber by Electrospray Deposition. High Polymers, Japan, Vol. 52, No.11 (2003) pp.829-832.

[6] Kawamoto, H., Electronic Circuit Printing, 3D printing and Film Formation Utilizing Electrostatic Inkjet Technology. DF2007: Digital Fabrication Processes Conference, Anchorage (2007) pp.961-964.

[7] O. A. Basaran. *Electrohydrodynamics of Drops and Bubbles*. PhD thesis, U. Minnesota U.S.A., 1983.

[8] O. A. Basaran and L. E. Scriven. Axisymmetric shapes and stability of pendant and sessile drops in an electric field. *J. Colloid Interface Sci.*, Vol. 140, pp. 10–30, 1990.

[9] M. T. Harris and O. A. Basaran. Capillary electrohydrostatics of conducting drops hanging from a nozzle in an electric field. *J. Colloid Interface Sci.*, Vol. 161, pp. 389–413, 1993.

[10] M. T. Harris and O. A. Basaran. Equillibrium shapes and stability of nonconducting pendant drops surrounded by a conducting fluid in an electric field. *J. Colloid Interface Sci.*, Vol. 170, pp. 308–319, 1995.

[11] T. Tsukada, M. Sato, N. Imaishi, M. Hozawa and K. Fujinawa. Static drop formation in an electrostatic field. *J. Chem. Eng. Jpn.*, Vol. 19, No. 6, pp. 537–542, 1986.

[12] Tada, K., Nishiura, M. and Kawamoto, H., Stability Anlysis of a Drop Generation from a Nozzle in an Electric Field., DF2008: Digital Fabrication Processes Conference, Pittsburgh (2008) pp.291-294.

[13] Kawamoto, H., Yasuda, H. and Umezu, S., Flow Distribution and Pressure of Air due to Ionic Wind in Pin-to-Plate Corona Discharge System., J. Electrostatics, Vol.64 (2006) pp.400-407.

[14] J. P. Abbott. An efficient algorithm for the determination of certain bifurcation points. *J. Comput. Appl. Math.*, Vol. 4, pp. 19–27, 1978.

[15] S. F. Kistler. *The fluid mechanics of certain coating and related viscous free-surface flows with contact lines*. PhD thesis, U. Minnesota U.S.A., 1984.

[16] G. Strang and G. J. Fix. *An Analysis of the Finite Element Method*. Prentice-Hall Inc., Englewood Cliffs, 1973.

Author Biography

Kazuyuki Tada started his professional career as an engineer in 1990 following completion of a M.S. degree at Keio University. Since then he has been working in a manufacturing engineering division of Fuji Xerox. From 1997 to 1999 he had a chance to study coating science and technology in University of Minnesota where he received another M.S. degree. During the stay in Minnesota, he participated in NIP14 at the first time as an audience in Toronto, CANADA. This is his fourth consecutive presentation at NIP/DF conference from 2008. Currently he enjoys double statuses of his career, a corporate engineer and a doctoral-course student at Waseda University.